Acta Mech 230, 2221–2231 (2019)
https://doi.org/10.1007/s00707-019-02382-2

ORIGINAL PAPER

W. Coenen · P. Rajamanickam · A. D. Weiss · A. L. Sánchez · F. A. Williams

Swirling flow induced by jets and plumes

Received: 11 September 2018 / Revised: 30 January 2019 / Published online: 21 March 2019

Abstract The interactions of the slow flow induced by the entrainment of axisymmetric jets and plumes with the surrounding geometry may result in the appearance of azimuthal swirling motion. This swirling flow evolves as it approaches the jet (or plume) as a result of the action of viscous forces on the solid surfaces bounding the fluid domain. When the initial size of the jet or plume a is much smaller than the characteristic radial distance R_∞ at which the swirl is generated, the evolution of the flow leads to a self-similar description with weak swirling motion, valid at intermediate radial distances R such that $a \ll R \ll R_\infty$ and axial distances L from the source such that $a \ll L \ll R_\infty$. In the present investigation of both laminar and turbulent jets and plumes, it is found that the circulation Γ is described by a self-similar solution of the second kind, with the exponent λ in the radial decay rate $\Gamma \propto (R/R_\infty)^\lambda$ obtained as an eigenvalue. The resulting azimuthal velocity distributions can find application in mathematical formulations of jet and plume problems involving interactions with ambient swirl, relevant in studies of dust devils and fire whirls.

1 Introduction

Swirling jets and plumes are central elements in a number of technological applications and natural phenomena. The interactions of the swirling motion with the streamwise motion play an important role in many interesting fluid-mechanical phenomena, an example being vortex breakdown [1,2], and are responsible for the emergence of tornadoes [3], dust devils [4], and fire whirls [5].

In technological applications pertaining to combustion, the swirling motion is imparted in the jet stream [6]. By way of contrast, in fire whirls the swirling motion is generated in the surrounding ambient atmosphere. Depending on the topography and wind conditions, different mechanisms can be responsible for the production of swirl in realistic scenarios, including flows channeled by topological features, interactions of multiple fires or plumes, or vortices formed in the wake of a hill or ridge [5]. In laboratory studies of dust devils and fire whirls, for example, the azimuthal velocity component is generated by the direct interaction of the relatively slow flow induced in the meridional plane by the entrainment of the developing plume with geometrical constraints placed at large radial distances. Different experimental arrangements are preferred by different groups, including a rotating cylindrical screen [7], a set of long vertical flow vanes placed at a certain angle with respect to the radial direction [8] and two slightly offset semi-cylindrical surfaces that leave two small slits for the tangential inflow of the entrained air [9].

The present analysis addresses the swirling motion induced in configurations, often found in experiments, where the constraints used to redirect the radial flow driven by entrainment are located at distances R_∞ much larger than the initial size of the jet or plume a (e.g., the injector radius of the jet or the size of the hot

W. Coenen (✉) · P. Rajamanickam · A. D. Weiss · A. L. Sánchez · F. A. Williams
Department of Mechanical and Aerospace Engineering, University of California, San Diego, 9500 Gilman Dr., La Jolla, CA 92093-0411, USA
E-mail: wicoenen@ucsd.edu

region generating the plume). Under those conditions, in a region where the axial distance from the source L is neither too small nor too large, such that $a \ll L \ll R_\infty$, the circulation Γ is expected to evolve for decreasing radial distances R to reach a solution at $a \ll R \ll R_\infty$ that is largely independent of the details of the swirl-generation process. Information about these intermediate solutions is essential in understanding the fluid-mechanical interactions occurring in the near field $R \sim a$ and in enabling rigorous mathematical formulations of the associated dust-devil and fire-whirl problems to be completed.

The analysis will consider laminar and turbulent jets and also laminar and turbulent plumes. At the edges of axisymmetric laminar plumes and of axisymmetric jets (laminar or turbulent), the entrainment rate per unit axial length (per azimuthal radian) Φ is constant and can be expressed in the form $\Phi = K\nu$, where ν is the kinematic viscosity of the fluid, but it varies with axial distance for turbulent plumes. The dimensionless entrainment constant K assumes values of order unity for laminar jets and also for laminar plumes, but it would be anticipated to be large for turbulent jets. When K is of order unity, the surrounding flow has an effective Reynolds number of order unity, as was shown by Schneider [10], who found an exact self-similar solution of the axisymmetric Navier–Stokes equations without circulation satisfying the no-slip condition at a circular-conical wall.

The Schneider solution was subsequently used in matched asymptotic expansions to construct higher-order descriptions of laminar jets [11] and also in a multiple-scale analysis to account for the slow momentum decay that occurs in the jet in the presence of the outer flow [12]. At large distances from the inlet, the jet has lost a significant fraction of its initial momentum, but the jet is still slender, and continues to entrain outer fluid with the same constant rate, up to extremely large distances from the jet exit that scale with the exponential of the jet Reynolds number squared. At these distances, the jet merges with the outer flow, giving rise to a large recirculating toroidal eddy whose description necessitates numerical integration of the full Navier–Stokes equations. The associated parameter-free problem has not been investigated yet, although an approximate description, obtained by extending the near-field asymptotic expansion outside its range of applicability, is given in [12,13], with results in agreement with experimental observations [14]. Since the length associated with jet momentum loss is typically many orders of magnitude larger than the characteristic size R_∞, this additional complicating effect does not need to be accounted for when analyzing the swirling motion induced by jets.

Schneider also considered the flow induced by turbulent jets [10], as well as the associated slow decay of the jet momentum flux [12], which has been observed in laboratory experiments [15]. The turbulent jet is bounded by a well-defined surface, across which the entrainment of non-turbulent fluid occurs [16], the flow induced in the surrounding atmosphere being laminar. Unlike laminar jets, however, the entrainment constant of a turbulent jet assumes a value $K \gg 1$ of the order of the jet Reynolds number, and the flow surrounding the jet is effectively inviscid and irrotational, outside a thin boundary layer located near the bounding wall. For axisymmetric turbulent plumes, the entrainment rate increases with the two-thirds power of the axial distance to the origin, and in the absence of swirl the surrounding flow also is potential outside a near-wall boundary layer. The potential-flow solutions describing the flow induced by turbulent jets and by turbulent plumes are due to Taylor [17].

These previous analyses did not consider the presence of azimuthal swirling motion, which is to be investigated here, with specific attention given to the intermediate-asymptotic solutions arising at distances $a \ll R \ll R_\infty$. After formulating the problem, we begin by considering the cases of laminar jets and laminar plumes. It is shown that the circulation, decreasing for decreasing radial distances R, is given by a self-similar solution of the second kind proportional to R^λ, with the exponent λ obtained as an eigenvalue. Solutions are also given for the self-similar swirling flow induced by a turbulent jet and (later) by a turbulent plume. In these cases, determination of the rate of radial decay requires consideration of the structure of the viscous flow in the near-wall boundary layer, such boundary layers not occurring in the fully viscous laminar problems.

2 Formulation

Although jets and plumes often emerge perpendicular to a flat wall, for generality our analysis considers the fluid domain to be bounded by a truncated conical wall of semi-angle $\pi - \alpha$, whose axis of symmetry is directed downstream along the jet or plume axis, as indicated in Fig. 1. Following Schneider, attention is given to angles $0 < \alpha < \pi$ with the case $\alpha = \pi/2$ representing the flow above a flat wall. Although the flow exiting from a straight pipe will be different in that the radius a plays an additional role, there nevertheless is some interest in the limit $\alpha = \pi$. The solution is described most conveniently in spherical polar coordinates (r, θ),

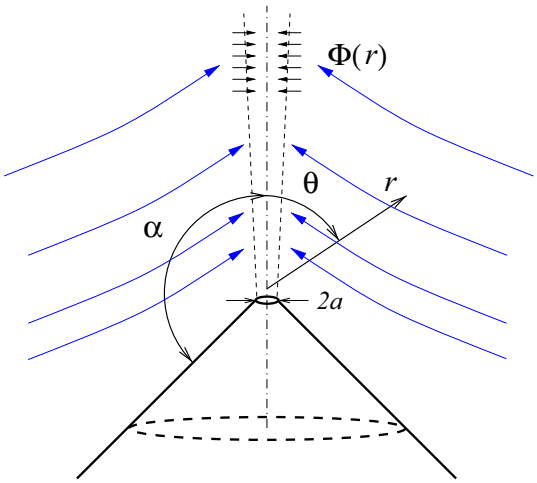

Fig. 1 Schematic illustration of the configuration and the adopted coordinate system

where $r = R/\sin\theta$ is the distance from the apparent apex of the cone and θ is the angular distance from the positive axis. For simplicity, in terms of the azimuthal component of velocity we introduce the circulation per unit azimuthal angle $\Gamma = r\sin\theta\, v_\varphi$ for describing the azimuthal swirling motion and employ the Stokes stream function ψ for the meridional motion, so that the radial and polar-angle components of velocity are

$$v_r = \frac{1}{r^2\sin\theta}\frac{\partial\psi}{\partial\theta} \quad \text{and} \quad v_\theta = -\frac{1}{r\sin\theta}\frac{\partial\psi}{\partial r}. \tag{1}$$

It is convenient to eliminate the pressure by writing the momentum equation in terms of the azimuthal component of the vorticity ω_φ, giving

$$\Omega = r\sin\theta\,\omega_\varphi = -\mathcal{L}(\psi), \tag{2}$$

involving the axisymmetric Stokesian operator,

$$\mathcal{L}() = \frac{\partial^2}{\partial r^2} + \frac{1-\xi^2}{r^2}\frac{\partial^2}{\partial\xi^2}, \tag{3}$$

where $\xi = \cos\theta$. In terms of the streamfunction and azimuthal vorticity, the axisymmetric Navier–Stokes equations governing the swirling motion reduce to

$$-\frac{\partial\psi}{\partial\xi}\frac{\partial}{\partial r}\left[\frac{\Omega}{r^2(1-\xi^2)}\right] + \frac{\partial\psi}{\partial r}\frac{\partial}{\partial\xi}\left[\frac{\Omega}{r^2(1-\xi^2)}\right] - \frac{1}{r^2(1-\xi^2)}\left(\frac{1}{r}\frac{\partial\Gamma^2}{\partial\xi} + \frac{\xi}{1-\xi^2}\frac{\partial\Gamma^2}{\partial r}\right) = \frac{\nu}{1-\xi^2}\mathcal{L}(\Omega), \tag{4}$$

$$-\frac{\partial\psi}{\partial\xi}\frac{\partial\Gamma}{\partial r} + \frac{\partial\psi}{\partial r}\frac{\partial\Gamma}{\partial\xi} = \nu r^2\mathcal{L}(\Gamma). \tag{5}$$

The set of boundary conditions for the far-field flow include the no-slip condition at the conical wall

$$\frac{\partial\psi}{\partial r} = 0,\ \frac{\partial\psi}{\partial\xi} = 0,\ \Gamma = 0 \quad \text{at} \quad \xi = \xi_w, \tag{6}$$

where $\xi_w = \cos\alpha$, together with the conditions along the axis of symmetry

$$\frac{\partial\psi}{\partial r} = \Phi,\ (1-\xi)^{1/2}\frac{\partial^2\psi}{\partial\xi^2} = 0,\ (1-\xi)^{1/2}\frac{\partial\Gamma}{\partial\xi} = 0 \quad \text{as} \quad \xi \to 1, \tag{7}$$

corresponding to matching with the velocity profile in the jet or plume, the quantity $\Phi = -r\sin\theta\, v_\theta$ representing the entrainment rate that may vary with the axial distance.

3 Swirling flow induced by laminar jets and laminar plumes

3.1 Schlichting and Yih velocity solutions

The structure of a submerged jet of initial radius a depends on the value of the Reynolds number $Re = (J/\pi)^{1/2}/\nu$, where J is the jet kinematic momentum flow rate (the integral of the square of the exit fluid volume flow rate over the jet exit area). For moderately large values of Re, the resulting slender laminar jet remains stable and can be calculated with errors of order Re^{-2} by integrating the boundary-layer form of the conservation equations. The solution includes a jet-development region with characteristic length $Re\, a$, which has been described numerically with the boundary-layer approximation in [18], followed by a self-similar region where the solution corresponds to the flow induced by a point source of momentum, obtained in closed analytical form by Schlichting [19]. The resulting stream function is given by $\psi = \nu r F_S(s)$, with

$$F_S = \frac{4s^2}{64/3 + s^2} \tag{8}$$

involving the rescaled transverse coordinate $s = Re\,\theta$. Since $-r \sin\theta v_\theta = \nu F_S$, as follows from Eq. (1), the entrainment rate is given in this case by $\Phi = \nu F_S(\infty) = 4\nu$.

As shown by Zel'dovich [20], the solution for laminar plumes far above the heat source (i.e., at distances sufficiently larger than the size of the heat source) can also be described using approximations of the boundary-layer type. The formulation of the self-similar problem, first written by Yih [21], involves the stream function $\psi = \nu r F_Y(y)$ and the similarity coordinate $y = (Br^2/\nu^3)^{1/4}\theta$, where B, widely termed the specific buoyant flux, is the (assumed constant) time rate of supply at the source of the weight (product of mass and acceleration of gravity) deficiency with respect to the ambient fluid (presumed to have constant density at the source level), divided by the ambient fluid density (resulting in units of B being the product of acceleration and volume per unit time) [22]. This supply rate at the source is a consequence of the axial force associated with the pressure gradient at the source differing from that in the ambient atmosphere. The solution depends on the Prandtl number Pr. With the exception of the two cases

$$F_Y = \frac{6y^2}{12\sqrt{2\pi} + y^2} \quad (Pr = 1) \quad \text{and} \quad F_Y = \frac{4y^2}{16\sqrt{2\pi/5} + y^2} \quad (Pr = 2), \tag{9}$$

the solution requires in general numerical integration [23]. The resulting constant entrainment rate $\Phi = K\nu$, with $K = F_Y(\infty)$, decreases with increasing Pr from the large value $K \simeq 5/Pr$ for $Pr \ll 1$ to reach a minimum value $K \simeq 3.2$ for $Pr \gg 1$ [24], with the intermediate values $K = 6$ and $K = 4$ corresponding to $Pr = 1$ and $Pr = 2$, respectively, as follows from Eq. (9).

3.2 Preliminary considerations

The flow induced in the surrounding atmosphere by the constant entrainment rate $\Phi = K\nu$ of self-similar laminar jets ($K = 4$) and plumes involves small characteristic velocities v_r and v_θ of order ν/r. Correspondingly, the presence of geometrical constraints at large radial distances $R \sim R_\infty \gg a$ can be expected to induce swirling velocities of order $v_\varphi \sim \nu/R_\infty$, corresponding to values of the circulation $\Gamma \sim \nu$. The specific distribution of Γ depends on the swirl-generation mechanism. For example, in experiments using vertical vanes to deflect the flow the inclination angle of the vanes with respect to the radial direction α determines the local value of the circulation $\Gamma = R_\infty(v_r \sin\theta + v_\theta \cos\theta)\tan\alpha$ in terms of the local velocity component perpendicular to the jet or plume $(v_r \sin\theta + v_\theta \cos\theta)$. We investigate below the existence of intermediate-asymptotic solutions for axial distances $a \ll L \ll R_\infty$, at radii $a \ll R \ll R_\infty$, independent of the specific details of the geometrical constraints that are responsible for redirecting the flow at $R \sim R_\infty$.

It is instructive to begin by investigating the existence of self-similar solutions of the first kind involving the velocity scalings $v_r \sim v_\theta \sim \nu/r$ and $\Gamma \sim \nu$, which apply in the swirl-generation region $R \sim R_\infty$. Introducing the self-similar stream function $\psi = K\nu r\tilde{f}(\xi)$ and associated circulation $\Gamma = K\nu h(\xi)$ into Eqs. (4) and (5) leads to

$$K^{-1}[(1-\xi^2)\tilde{f}'''' - 4\xi\tilde{f}'''] - \tilde{f}\tilde{f}''' - 3\tilde{f}'\tilde{f}'' - 2hh'/(1-\xi^2) = 0, \tag{10}$$

$$K^{-1}(1-\xi^2)h'' - \tilde{f}h' = 0, \tag{11}$$

to be integrated with the boundary conditions

$$\begin{cases} \tilde{f} = \tilde{f}' = h = 0 & \text{at } \xi = \xi_w, \\ \tilde{f} - 1 = (1-\xi)^{1/2}\tilde{f}'' = (1-\xi)^{1/2}h' = 0 & \text{as } \xi \to 1. \end{cases} \tag{12}$$

In the notation employed throughout the paper, the prime denotes differentiation of functions of one variable (for example, differentiation with respect to ξ in the above equations).

It is found that the solution to the above problem involves necessarily a zero circulation $h = 0$. To see this, one may integrate Eq. (11) once to write

$$h'(\xi) = h'(\xi_w)\exp\left(\int_{\xi_w}^{\xi} \frac{K\tilde{f}(x)}{1-x^2}\mathrm{d}x\right). \tag{13}$$

The integrand in the exponential is non-integrable as $\xi \to 1$. Therefore, for any finite-valued function $\tilde{f}(\xi)$ satisfying Eq. (12), the slope at the wall $h'(\xi_w)$ must vanish in order to satisfy the analyticity condition at the axis of symmetry, so that $h'(\xi)$ is identically zero everywhere, as follows from Eq. (13). Since only solutions with constant h are admissible, consideration of the no-slip condition at $\xi = \xi_w$ leads to the anticipated result $h = 0$, while the solution for $\tilde{f}$ reduces to Schneider's stream function f, obtained by integrating

$$K^{-1}[(1-\xi^2)f'''' - 4\xi f'''] - ff''' - 3f'f'' = 0 \tag{14}$$

with boundary conditions

$$\begin{array}{ll} f = f' = 0 & \text{at } \xi = \xi_w, \\ f - 1 = (1-\xi)^{1/2}f'' = 0 & \text{as } \xi \to 1. \end{array} \tag{15}$$

3.3 The self-similar solution of the second kind

The above considerations indicate that the magnitude of the circulation Γ at intermediate distances $a \ll R \ll R_\infty$ is negligible compared with ν. Hence, the motion in the meridional plane, with characteristic velocities $v_r \sim v_\theta \sim \nu/r$ given by Schneider's stream function $\psi = K\nu r f(\xi)$, is accompanied by a much weaker swirling motion, whose magnitude decays with decreasing radial distance as a result of the action of the viscous forces on the wall. The associated solution for the circulation is a self-similar solution of the second kind [25] of the form

$$\Gamma = Ar^{\lambda}\Lambda(\xi), \tag{16}$$

where the exponent $\lambda > 0$ and the function $\Lambda(\xi)$, defining the rate of radial decay and the angular distribution of the azimuthal swirl, respectively, are determined by solving the eigenvalue problem

$$\left.\begin{array}{l} K^{-1}[(1-\xi^2)\Lambda'' + \lambda(\lambda-1)\Lambda] - f\Lambda' + \lambda f'\Lambda = 0 \\ \Lambda = 0 \text{ at } \xi = \xi_w; \quad (1-\xi)^{1/2}\Lambda' \to 0 \text{ as } \xi \to 1 \end{array}\right\} \tag{17}$$

as follows from Eq. (5). Without loss of generality, in looking for nontrivial solutions of Eq. (17) the normalization condition $\Lambda(1) = 1$ is added to the computation of Λ. As is common in self-similar solutions of the second kind [25], the constant factor $A \sim \nu/R_\infty^{\lambda}$ defining in Eq. (16) the magnitude of the circulation, whose value depends on the details of the swirl-generation process occurring at $R \sim R_\infty$, remains undetermined in the analysis.

The self-similar structure identified here is reminiscent of that encountered previously in connection with the axisymmetric flow surrounding a swirling jet discharging into a cylindrical coaxial confinement [26]. For that configuration, the surrounding recirculating flow exhibits near the backstep wall a self-similar solution of the first kind for the radial and axial velocity components and a self-similar solution of the second kind for the azimuthal velocity, with a constant factor corresponding to A in the above description affecting the latter, determined in that case by matching with the numerical solution found in the main recirculating region.

The solution of the eigenvalue problem defined in Eq. (17), obtained numerically by a shooting method with an expansion of the solution about $\xi = 1$ employed to begin the integration and the value of λ adjusted iteratively to satisfy the first boundary condition in Eq. (17), depends on the entrainment constant K and on the angle α. Nontrivial solutions exist for a discrete set of positive values of λ. Since larger values of λ correspond to swirl velocities that decay at a faster rate with decreasing radial distances, the eigenmode with the smallest

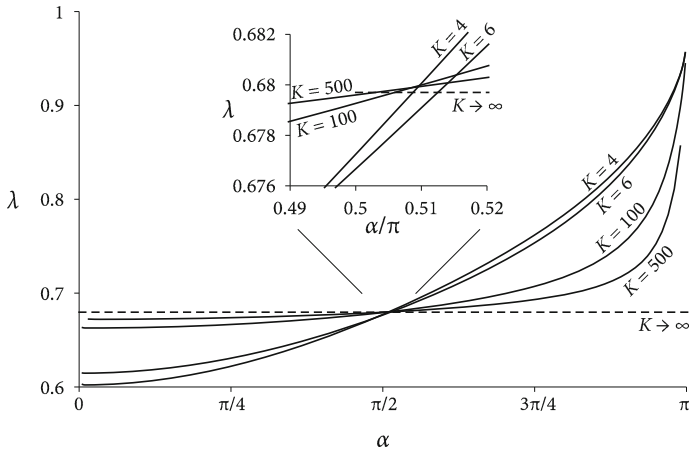

Fig. 2 The exponent λ of the radial decay rate of the circulation as a function of the angle α, for various values of the dimensionless entrainment constant K

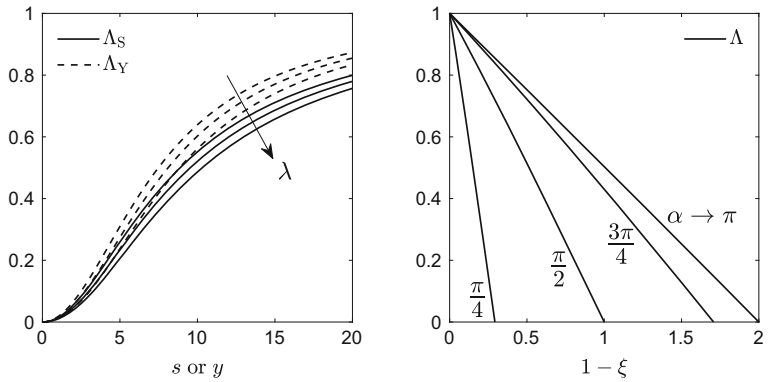

Fig. 3 Left: transverse distributions of circulation inside the laminar jet (Λ_S) and the laminar plume with $Pr = 1$ (Λ_Y) obtained from integration of Eqs. (18) and (19) for three values of $\lambda = (0.68, 0.8, 0.95)$. Right: profiles of self-similar circulation $\Lambda(\xi)$ obtained by integration of Eq. (17) with $K = 4$ for different values of α

eigenvalue ultimately dominates the azimuthal motion as the axis is approached, so it is this value that is shown in Fig. 2. It is seen that λ increases with increasing α and is not very sensitive to changes in K, especially near the planar-wall value $\alpha = \pi/2$, where the resulting differences in λ are quite small, as is shown in an inset. The eigenfunctions Λ corresponding to the leading eigenvalues plotted in Fig. 2 decrease monotonically with increasing θ. The resulting distributions, almost linear in the coordinate $\xi = \cos\theta$, are shown on the right-hand side of Fig. 3 for $K = 4$, corresponding to a laminar jet or a laminar plume with $Pr = 2$.

3.4 Jet and plume swirl structures and uniformly valid solutions

The previous analysis provides in particular the axial distribution $\Gamma = Ar^{\lambda}$ along $\theta = 0$, corresponding to the circulation surrounding the jet or plume. Since the circulation vanishes at the axis, the azimuthal velocity must evolve across the jet or plume rapidly compared with its rate of change outside. The resulting distribution of Γ is determined by integrating Eq. (5), employing convective terms evaluated with the corresponding self-similar velocity. For the plume, a solution for $\lambda = 0$, corresponding to constant circulation in the surrounding atmosphere, was obtained by Thomas and Takhar [27]. We give here solutions for values $\lambda > 0$ corresponding to our self-similar distributions.

For the jet, described by the similarity coordinate $s = Re\,\theta$, the solution for the circulation $\Gamma = Ar^{\lambda}\Lambda_S(s)$ is obtained by integration of

$$s\Lambda_S'' + (F_S - 1)\Lambda_S' - \lambda F_S'\Lambda_S = 0; \quad \Lambda_S(0) = \Lambda_S(\infty) - 1 = 0, \tag{18}$$

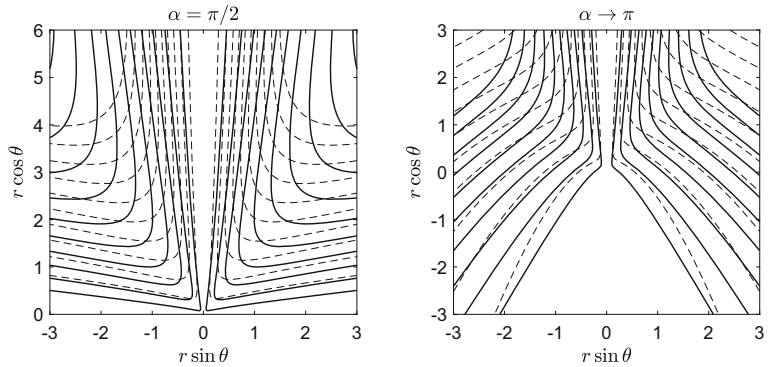

Fig. 4 Streamlines (dashed curves) and iso-contours of circulation (solid curves) corresponding to a laminar jet with $Re = 20$ as obtained for $\alpha = \pi/2$ and $\alpha \to \pi$ from the uniformly valid composite expansions given in Eqs. (20) and (22). Results are given for equally spaced values of the dimensionless stream function ψ/ν ranging from $\psi/\nu = 1$ (bottom curve) to $\psi/\nu = 12$ (top curve) and also for equally spaced values of the circulation $\Gamma/A = 0.1-1.5$

where F_S is the Schlichting stream function shown in Eq. (8). Similarly, for the plume the distribution of circulation $\Gamma = Ar^\lambda \Lambda_Y(y)$ is obtained in terms of the transverse coordinate $y = (Br^2/\nu^3)^{1/4}\theta$ from

$$y\Lambda_Y'' + (F_Y - 1)\Lambda_Y' - \lambda F_Y'\Lambda_Y = 0; \quad \Lambda_Y(0) = \Lambda_Y(\infty) - 1 = 0, \tag{19}$$

where $F_Y(y)$ is Yih's stream function [21], given in Eq. (9) for $Pr = 1$ and $Pr = 2$. For $\lambda = 0$, this equation reduces to the equation for constant outer circulation, considered in [27], as it must.

The self-similar solutions for the circulation inside laminar jets or laminar plumes are plotted on the left-hand side of Fig. 3 for three selected relevant values of the eigenvalue λ. These results can be combined with the circulation in the surrounding atmosphere to construct the composite expansions

$$\Gamma = Ar^\lambda[\Lambda(\cos\theta) + \Lambda_S(Re\,\theta) - 1] \tag{20}$$

for the jet and

$$\Gamma = Ar^\lambda[\Lambda(\cos\theta) + \Lambda_Y(B^{1/4}r^{1/2}\theta/\nu^{3/4}) - 1] \tag{21}$$

for the plume. These expressions, together with the composite expansion for the stream function obtained previously by Schneider [10], provide a uniformly valid description for the far-field velocity of laminar jets and laminar plumes. Sample results are shown in Fig. 4 for a jet with $Re = 20$, including the streamlines (dashed curves), evaluated from the expression

$$\psi/\nu = 4r\left[\frac{(Re\,\theta)^2}{64/3 + (Re\,\theta)^2} + f(\cos\theta) - 1\right]. \tag{22}$$

4 Swirling flow induced by turbulent jets

In the absence of swirl, turbulent jets are known to display a self-similar solution including a mean mass flow rate that increases linearly with distance, corresponding to a constant entrainment rate. In this case, however, the entrainment rate $\Phi = K\nu$ is proportional to the square root of the kinematic momentum flow rate of the jet J, yielding $K \propto Re \gg 1$ [28]. This linear proportionality has been verified in direct experimental measurements of entrainment [29], with the resulting constant of proportionality being somewhat smaller than that predicted theoretically by combining a simple turbulence model with measurements of the jet width [28]. Because of the large value of the entrainment rate, the solution for the induced flow can be obtained by taking the limit $K \gg 1$ in Eq. (14). Integration of the resulting equation subject to $f(1) - 1 = f(\xi_w) = 0$ yields Taylor's potential solution [17] $f = (\xi - \xi_w)/(1 - \xi_w)$. Effects of viscous forces are confined to a thin near-wall boundary layer of characteristic thickness $K^{-1/2} \ll 1$, which can be described by introducing the rescaled variables

$$\eta = \frac{K^{1/2}(\xi - \xi_w)}{(1 - \xi_w)(1 + \xi_w)^{1/2}} \tag{23}$$

and

$$F = \frac{K^{1/2} f}{(1+\xi_w)^{1/2}}, \tag{24}$$

yielding the parameter-free problem

$$F''' - FF'' + 1 - F'^2 = 0, \quad \begin{cases} F = F' = 0 & \text{at } \eta = 0, \\ F' \to 1 & \text{as } \eta \to \infty. \end{cases} \tag{25}$$

The presence of swirl requires in principle modifications to the above solution. In the large-Reynolds-number flow that surrounds the turbulent jet, the circulation is conserved along streamlines, as follows from Eq. (5), so that the spatial distribution of circulation necessarily depends on the specific manner in which swirl is introduced in the far field. If the resulting circulation is non-uniform, then azimuthal-vorticity production through vortex-line stretching becomes important, as seen in Eq. (4), with the result that the flow in the meridional plane differs in general from that described by Taylor's potential solution. The resulting flow, which lacks in general a self-similar solution, includes a viscous boundary layer where the radial pressure gradient associated with the swirling motion can be expected to induce a strong radial inflow, thereby complicating further the flow structure. For example, Burggraf, Stewartson, and Belcher [30] have shown that a potential vortex with its axis perpendicular to a flat wall induces a viscous boundary layer on the wall that grows as the radius decreases, reaches a maximum thickness, then decreases to zero thickness when the radius reaches zero, thereby generating azimuthal vorticity in the flow external to the boundary layer as the axis is approached.

The previous discussion suggests that the swirling motion induced by turbulent jets exhibits in general a complicated structure at intermediate radial distances $a \ll R \ll R_\infty$, including regions lacking a self-similar solution that require numerical integration of partial differential equations to obtain proper matching conditions. The solution simplifies in configurations where the flow deflection from the radial direction at the external boundary is small, leading to weak swirl. If the deflection does not involve generation of azimuthal vorticity, then the inviscid outer flow remains irrotational everywhere, and the meridional motion is given by Taylor's potential solution [17] $f = (\xi - \xi_w)/(1 - \xi_w)$ at intermediate radial distances $a \ll R \ll R_\infty$, whereas the self-similar structure of the accompanying viscous boundary layer is described by Eq. (25). Even in this case of weak swirl, self-similar solutions of the form $\Gamma = Ar^\lambda \Lambda(\xi)$, analogous to those identified above for laminar jets and plumes, can be encountered only in special cases, for which it can be seen by integrating Eq. (17) for $K \gg 1$ that

$$\Lambda = \left(\frac{\xi - \xi_w}{1 - \xi_w}\right)^\lambda \tag{26}$$

in the outer inviscid region. Since this self-similar solution must be compatible with the distribution of swirl introduced at the external boundary, its existence requires that the swirl-generation mechanism be adjusted to produce exactly the needed circulation distribution. That special case, a notably simple one, is the case considered here, and a corresponding simplification will be addressed for turbulent plumes in the following section. It is important to recognize this limitation and to realize that alternative analyses of swirling turbulent jets and plumes are warranted in the future.

The exponent λ in the self-similar solution $\Gamma = Ar^\lambda \Lambda(\xi)$ is determined in this case by considering the distribution of circulation in the boundary layer, given by the solution to the eigenvalue problem

$$\Lambda'' - F\Lambda' + \lambda F' \Lambda = 0, \quad \begin{cases} \Lambda = 0 & \text{at } \eta = 0, \\ \eta\Lambda' - \lambda\Lambda \to 0 & \text{as } \eta \to \infty, \end{cases} \tag{27}$$

independent of α. This mathematical problem was encountered earlier in [30] when describing the circulation in the near-wall viscous sublayer induced by a potential vortex. The eigenvalue was found to be $\lambda = 0.6797$, with associated distributions of $F(\eta)$ and $\Lambda(\eta)$ shown as dashed curves in Fig. 5.

The prediction $\lambda = 0.6797$ for $K \to \infty$, represented by a horizontal dashed line in Fig. 2, can be compared with the values of λ obtained for finite values of $K \gg 1$ by integration of the eigenvalue problem defined in Eq. (17). As can be seen, although the value of λ tends to approach $\lambda = 0.6797$ for increasing K, the departures remain significant for configurations with cone angles approaching $\alpha = \pi$ (i.e., values of $\xi_w \to -1$). As can be anticipated from Eqs. (23) and (24), investigation of cases with $1 + \xi_w \ll 1$ requires introduction of rescaled boundary-layer variables. In the distinguished limit $K^{-1} \sim 1 + \xi_w$, the selections

$$\gamma = K(\xi - \xi_w) \quad \text{and} \quad \tilde{F} = 2Kf \tag{28}$$

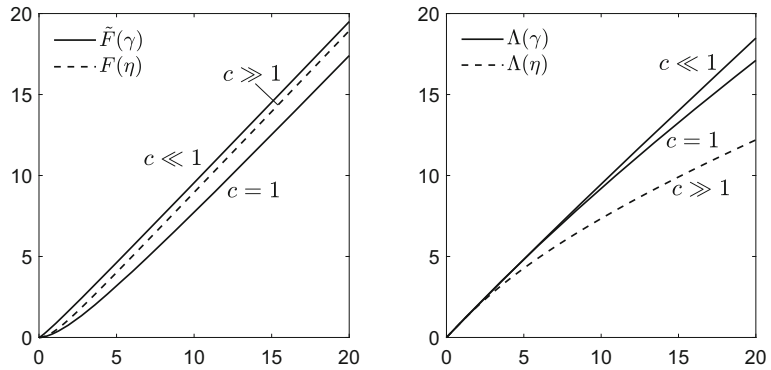

Fig. 5 Self-similar stream function and circulation inside boundary layer for turbulent jets. Dashed curves correspond to integration of Eqs. (25) and (27), whereas the solid curves are obtained from Eqs. (29) and (30)

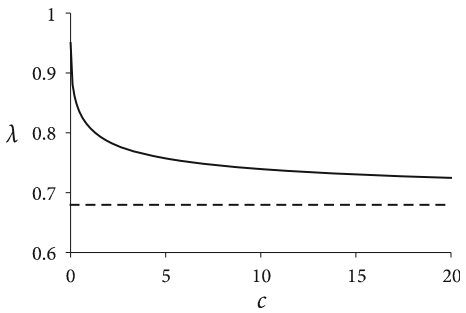

Fig. 6 The variation with $c = K(1+\xi_w)$ of the eigenvalue λ obtained from Eq. (30) for turbulent jets with $K^{-1} \sim 1+\xi_w \ll 1$

are seen to yield the modified problem

$$4[(\gamma+c)\tilde{F}'']' - \tilde{F}\tilde{F}'' + 1 - \tilde{F}'^2 = 0, \quad \begin{cases} \tilde{F} = \tilde{F}' = 0 & \text{at } \gamma = 0, \\ \tilde{F}' \to 1 & \text{as } \gamma \to \infty, \end{cases} \tag{29}$$

and

$$4(\gamma+c)\Lambda'' - \tilde{F}\Lambda' + \lambda\tilde{F}'\Lambda = 0, \quad \begin{cases} \Lambda = 0 & \text{at } \gamma = 0, \\ \gamma\Lambda' - \lambda\Lambda \to 0 & \text{as } \gamma \to \infty, \end{cases} \tag{30}$$

where $c = K(1+\xi_w)$ carries the dependence of the problem on K and α. Sample profiles of stream function $\tilde{F}$ and circulation Λ are shown in Fig. 5, while the variation of λ with c is given in Fig. 6. In agreement with the results for $K = 100$ and $K = 500$ shown in Fig. 2, which give values of λ increasing as α approaches π, the value of λ obtained from Eq. (30) decreases with increasing c, asymptotically approaching for $c \gg 1$ the limiting value $\lambda = 0.6797$ corresponding to the prediction for $K \to \infty$.

5 Swirling flow induced by turbulent plumes

As can be shown on the basis of dimensional arguments [22], for turbulent plumes the mass flow rate in the far field is proportional to $r^{5/3}$, consistent with an entrainment rate increasing with $r^{2/3}$ [31]. This can be expressed in the form $\Phi = (5/3)CB^{1/3}r^{2/3}$ in terms of the specific buoyancy flux B and a dimensionless order-unity constant $(5/3)C$, the latter including an inconsequential factor $5/3$ that simplifies the following expressions for the stream function. In the absence of swirl, the flow induced is inviscid and potential, as described by Taylor [17], except in a near-wall boundary layer whose thickness is proportional to $r^{-1/3}$. In the inviscid region, the stream function takes the self-similar form $\psi = CB^{1/3}r^{5/3}g(\xi)$, where the function g is determined by integration of

$$(1-\xi^2)g'' + \frac{10}{9}g = 0; \quad g(\xi_w) = g(1) - 1 = 0. \tag{31}$$

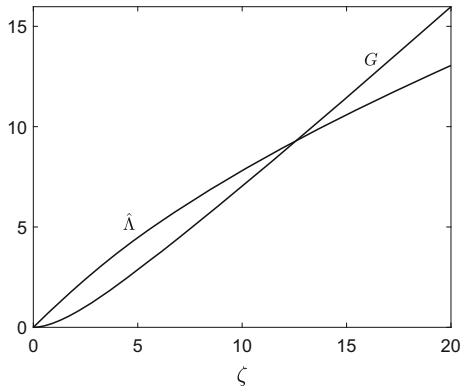

Fig. 7 Self-similar stream function G and circulation $\hat{\Lambda}$ inside the near-wall boundary layer obtained from integration of Eqs. (35) and (37) for the case of turbulent plumes

The solution is

$$g = \frac{\pi}{\sqrt{3}}\sqrt{1-\xi^2}\left[\frac{P^1_{2/3}(-\xi_w)}{P^1_{2/3}(\xi_w)}P^1_{2/3}(\xi) - P^1_{2/3}(-\xi)\right], \tag{32}$$

where $P^1_{2/3}$ is the associated Legendre function of the first kind, with degree $2/3$ and order 1. As previously indicated, this is the special case to be addressed here for our swirling flows. Note that the specific expressions given by Taylor [17] for the cases $\alpha = \pi/2$ and $\alpha = \pi$, involving derivatives of Legendre functions of degree $2/3$, can be readily recovered from the general solution given in Eq. (32) by using the fact that the associated Legendre function of order m can be expressed in terms of the mth derivative of the Legendre function of the same degree.

Near the bounding wall, the solution is of the form $g = (\xi - \xi_w)g'_w$, where

$$g'_w = g'(\xi_w) = \frac{-2\pi}{3\sqrt{3}\sqrt{1-\xi_w^2}}\left[\frac{P^1_{2/3}(-\xi_w)}{P^1_{2/3}(\xi_w)}P^1_{5/3}(\xi_w) + P^1_{5/3}(-\xi_w)\right], \tag{33}$$

($g'_w \neq 0$ for all α), thereby yielding a nonzero slip velocity $v_r = -CB^{1/3}g'_w r^{-1/3}$. If the circulation in the potential region is assumed to be proportional to r^λ with $\lambda > 2/3$, then straightforward integration of the inviscid form of Eq. (5) yields

$$\Gamma = Dr^\lambda g^{3\lambda/5}, \tag{34}$$

where $D \sim B^{1/3}R_\infty^{2/3-\lambda}$ is an unknown constant whose value carries information of the far-field region $R \sim R_\infty$. As in the case of turbulent jets, the exponent λ is obtained by consideration of the boundary-layer region.

In the boundary layer, the stream function can be rewritten in the form $\psi = [CB^{1/3}\nu g'_w(1-\xi_w^2)]^{1/2}r^{4/3}G(\zeta)$, where the function G satisfies the boundary-value problem,

$$G''' - \frac{4}{3}GG'' + \frac{1}{3}(1-G'^2) = 0; \quad G(0) = G'(0) = G'(\infty) - 1 = 0, \tag{35}$$

with the prime denoting here differentiation with respect to the rescaled coordinate $\zeta = [g'_w/(1-\xi_w^2)]^{1/2}(CB^{1/3}/\nu)^{1/2}r^{1/3}(\xi - \xi_w)$. The circulation inside the boundary layer can be expressed in the form

$$\Gamma = Dr^{4\lambda/5}[g'_w(1-\xi_w^2)\nu/(CB^{1/3})]^{3\lambda/10}\hat{\Lambda}(\zeta) \tag{36}$$

in terms of the similarity function $\hat{\Lambda}(\zeta)$, which satisfies

$$\hat{\Lambda}'' - \frac{4}{3}G\hat{\Lambda}' + \frac{4}{5}\lambda G'\hat{\Lambda} = 0, \quad \begin{cases} \hat{\Lambda} = 0 & \text{at } \zeta = 0, \\ \zeta\hat{\Lambda}' - \frac{3}{5}\lambda\hat{\Lambda} \to 0 & \text{as } \zeta \to \infty. \end{cases} \tag{37}$$

The smallest eigenvalue describing the circulation is found to be $\lambda = 1.0453$. For completeness, the solutions of the boundary-value problems given in Eqs. (35) and (37) are shown in Fig. 7.

6 Concluding remarks

The analyses of the four swirling-flow problems that have been presented here offer further illustrations of ways in which considerations of intermediate asymptotics may result in self-similar solutions of the second kind. The scaling considerations that were required help to clarify the range of swirling-flow conditions that may be encountered under different circumstances. The complex flow fields that occur in the vicinity of swirl-producing vanes have been shown to evolve to self-similar flows that persist over most of the intermediate region, where the radial distance from the source location is small compared with the radius of the swirl-producing devices but large compared with the size of the source. The range of circulation treated here is of the order of the kinematic viscosity of the fluid, with augmentation by the jet Reynolds number or by the plume Grashof number (the latter expressed through the buoyancy flux in the analysis). It would be of interest to investigate other possible scalings for which different flow regimes may arise. Such future investigations might expand our comprehension of swirling-flow phenomena beyond the present knowledge.

Acknowledgements We thank a referee for constructive comments.

References

1. Hall, M.G.: Vortex breakdown. Ann. Rev. Fluid Mech. **4**, 195–218 (1972)
2. Leibovich, S.: The structure of vortex breakdown. Ann. Rev. Fluid Mech. **10**, 221–246 (1978)
3. Fujita, T.T.: Tornadoes around the world. Weatherwise **26**, 56–83 (1973)
4. Maxworthy, T.: A vorticity source for large-scale dust devils and other comments on naturally occurring columnar vortices. J. Atmos. Sci. **30**, 1717–1722 (1973)
5. Tohidi, A., Gollner, M.J., Xiao, H.: Fire whirls. Ann. Rev. Fluid Mech. **50**, 187–213 (2018)
6. Candel, S., Durox, D., Schuller, T., Bourgouin, J.F., Moeck, J.P.: Dynamics of swirling flames. Ann. Rev. Fluid Mech. **46**, 147–173 (2014)
7. Emmons, H.W., Ying, S.-J.: The fire whirl. Proc. Combust. Inst. **11**, 475–488 (1967)
8. Mullen, J.B., Maxworthy, T.: A laboratory model of dust devil vortices. Dyn. Atmos. Oceans **1**, 181–214 (1977)
9. Byram, G.M., Martin, R.E.: Fire whirl-winds in the laboratory. Fire Control Notes **23**, 13–17 (1962)
10. Schneider, W.: Flow induced by jets and plumes. J. Fluid Mech. **108**, 55–65 (1981)
11. Mitsotakis, K., Schneider, W., Zauner, E.: Second-order boundary-layer theory of laminar jet flows. Acta Mech. **53**, 115–123 (1981)
12. Schneider, W.: Decay of momentum flux in submerged jets. J. Fluid Mech. **154**, 91–110 (1985)
13. Schneider, W., Zauner, E., Böhm, H.: The recirculatory flow induced by a laminar axisymmetric jet issuing from a wall. J. Fluids Eng. **109**, 237–241 (1987)
14. Zauner, E.: Visualization of the viscous flow induced by a round jet. J. Fluid Mech. **154**, 111–119 (1985)
15. Sforza, P.M., Mons, R.F.: Mass, momentum, and energy transport in turbulent free jets. Int. J. Heat Mass Transf. **21**, 371–384 (1978)
16. Townsend, A.A.: The Structure of Turbulent Shear Flow. Cambridge University Press, Cambridge (1976)
17. Taylor, G.I.: Flow induced by jets. J. Aero/Space Sci. **25**, 464–465 (1957)
18. Revuelta, A., Sánchez, A.L., Liñán, A.: The virtual origin as a first-order correction for the far-field description of laminar jets. Phys. Fluids **14**, 1821–1824 (2002)
19. Schlichting, H.: Laminare Strahlausbreitung. Z. Angew. Math. Mech. **13**, 260–263 (1933)
20. Zel'dovich, Y.B.: The asymptotic laws of freely-ascending convective flows. Zhur. Eksper. Teor. Fiz **7**, 1463–1465 (1937)
21. Yih, C.S.: Free convection due to a point source of heat. In: Proceedings of the First US National Congress of Applied Mechanics, pp. 941–947 (1951)
22. Turner, J.S.: Buoyant plumes and thermals. Annu. Rev. Fluid Mech. **1**, 29–44 (1969)
23. Fujii, T.: Theory of the steady laminar natural convection above a horizontal line heat source and a point heat source. Int. J. Heat Mass Transf. **6**, 597–606 (1963)
24. Kurdyumov, V.N., Liñán, A.: Free convection from a point source of heat, and heat transfer from spheres at small Grashof numbers. Int. J. Heat Mass Transf. **42**, 3849–3860 (1999)
25. Barenblatt, G.I., Zel'dovich, Y.B.: Self-similar solutions as intermediate asymptotics. Annu. Rev. Fluid Mech. **4**, 285–312 (1972)
26. Revuelta, A., Sánchez, A.L., Liñán, A.: Confined swirling jets with large expansion ratios. J. Fluid Mech. **508**, 89–98 (2004)
27. Thomas, T.G., Takhar, H.S.: Swirling motion in a buoyant plume. Acta Mech. **71**, 185–193 (1988)
28. Schlichting, H., Gersten, K.: Boundary-Layer Theory, 9th edn, pp. 672–673. Springer, Berlin (2017)
29. Ricou, F.P., Spalding, D.B.: Measurements of entrainment by axisymmetrical turbulent jets. J. Fluid Mech. **11**, 21–32 (1961)
30. Burggraf, O.R., Stewartson, K., Belcher, R.: Boundary layer induced by a potential vortex. Phys. Fluids **14**, 1821–1833 (1971)
31. Batchelor, G.K.: Heat convection and buoyancy effects in fluids. Q. J. R. Meteorol. Soc. **80**, 339–358 (1954)